The Astrophysical Journal Letters, 915:L33 (8pp), 2021 July 10 https://doi.org/10.3847/2041-8213/ac0f81

Stars Lensed by the Supermassive Black Hole in the Center of the Milky Way: Predictions for ELT, TMT, GMT, and JWST

Michał J. Michałowski[1] and Przemek Mróz[2]
[1] Astronomical Observatory Institute, Faculty of Physics, Adam Mickiewicz University, ul. Słoneczna 36, 60-286 Poznań, Poland; mj.michalowski@gmail.com
[2] Division of Physics, Mathematics, and Astronomy, California Institute of Technology, Pasadena, CA 91125, USA
Received 2021 June 17; revised 2021 June 27; accepted 2021 June 29; published 2021 July 14

Abstract

Gravitational lensing is an important prediction of general relativity, providing both its test and a tool to detect faint but amplified sources and to measure masses of lenses. For some applications, (e.g., testing the theory), a point source lensed by a point-like lens would be more advantageous. However, until now only one gravitationally lensed star has been resolved. Future telescopes will resolve very small lensing signatures for stars orbiting the supermassive black hole (SMBH) in the center of the Milky Way. The lensing signatures, however, should be easier to detect for background stars. We predict that the Extremely Large Telescope (ELT), Thirty Meter Telescope (TMT), and Giant Magellan Telescope (GMT) will resolve the lensed images of around 100 (60) stars in the disk and 30 (20) stars in the bulge in the background of the SMBH, down to 28 (27) mag (Vega) limits at *K*-band, requiring 5 (1) hr of integration. In order to detect several such stars one needs the limit of at least 24 mag. With decade-long monitoring, one can also detect the rotation of the lensed images. The detection of elongated images will not be possible, because this would require a nearly perfect source-lens alignment. The James Webb Space Telescope (JWST) will likely be limited by the confusion caused by stars near the Galactic center. The detection of such lensed images will provide a very clean test of general relativity, when combined with the SMBH mass measurement from orbital motions of stars, and accurate measurements of the SMBH properties, because both the source and the lens can be considered point-like.

Unified Astronomy Thesaurus concepts: Optical telescopes (1174); Galactic center (565); Supermassive black holes (1663); Strong gravitational lensing (1643)

1. Introduction

Gravitational lensing is an important prediction of general relativity, providing both the test of the theory and a tool to detect faint but amplified sources and to measure masses also for lenses not detected by other means. The first confirmation of this effect came from the measurement of the displacement of star positions close to the Solar limb during a Solar eclipse (Dyson et al. 1920). Then, numerous examples of strong gravitational lensing with multiple images, arcs, and rings were reported for lensed galaxies. In these cases the lenses and sources are extended and complex objects. For some applications, for example testing of general relativity, a point source lensed by a point-like lens (as already described by Chwolson 1924 and Einstein 1936) would be more advantageous. However, until now only one star gravitationally lensed by another star has been resolved into lensed images (Dong et al. 2019). This is because for a stellar lens (or a less massive object) the Einstein radius is too small to be resolved with current instrumentation, a problem already noted by Einstein (1936). Lensing caused by stellar- and planetary-mass objects was detected many times with unresolved but amplified images of background stars, a phenomena called microlensing (Paczynski 1986, 1996; Udalski et al. 1993, 2005; Wyrzykowski et al. 2015; Mróz et al. 2017, 2018; Wyrzykowski & Mandel 2020).

For a galaxy lens, a background star is too faint to be detected and distinguished from its host galaxy. Indeed, this was successful only for four stars (at $z = 0.5$–2) lensed by clusters of galaxies or individual galaxies: the Refsdal supernova lensed into an Einstein cross and a delayed fifth image, predicted before its appearance (Kelly et al. 2015, 2016; Diego et al. 2016; Grillo et al. 2016; Jauzac et al. 2016), two other supernovae (Goobar et al. 2017; Rodney et al. 2021), and a blue supergiant with a possible detection of a secondary image (Kelly et al. 2018).

A possibility to resolve a lensed image of an individual star is offered by the supermassive black hole (SMBH) in the center of the Milky Way, because it is massive and close enough for the Einstein ring to be resolved for some stars behind it. From the motion of stars around the SMBH, its mass was measured to be $4 \times 10^6\,M_\odot$ (Eckart & Genzel 1996, 1997; Genzel et al. 1996, 1997, 2000; Ghez et al. 1998, 2000, 2005, 2008; Eckart et al. 2002). However, even with this mass, the lensing of the orbiting stars is difficult to detect. The star S87 has the widest orbit explored so far with the semimajor axis of 2.″74 (Gillessen et al. 2017). This corresponds to a maximum distance behind the SMBH of 0.05 pc or 10,000 au. At such a distance the Einstein radius is only 5 mas, an order of magnitude smaller than the best resolution currently achievable in the optical for stars as faint as those orbiting the SMBH. Moreover, detecting lensing signatures would require a near-perfect alignment of a star with the direction toward the SMBH.

Future telescopes will reach resolutions that are sufficient to resolve such small lensing signatures. Bozza & Mancini (2009) predicted that in 2062 the secondary lensed images of stars S6 and S27 will reach 20–22 mag at a separation of 0.3–0.4 mas from the shadow of the SMBH (see also Wardle & Yusef-Zadeh 1992; Jaroszynski 1998; De Paolis et al. 2003; Bozza & Mancini 2004, 2005; Bin-Nun 2010). In 2047 the secondary image of star S14 will reach 23.5 mag 0.14 mas away. Bozza & Mancini (2012) also considered the possibility of detecting astrometric shifts of the primary images of orbiting stars due to lensing, with expected values of up to 0.3 mas. There is also a possibility of detecting the amplification of stars behind the

SMBH, but at the current sensitivity limit these events are rarer than one per century (Alexander & Sternberg 1999).

The lensing signatures, however, should be stronger and easier to detect for background stars. The Einstein radius is 0.″7, 1.″4, and 1.″6 for a star 1, 8, and 16 kpc behind the SMBH, respectively. Therefore, major limitation is not the resolution directly, but confusion caused by stars in the Galactic center and the number density of distant stars that could align almost perfectly with the SMBH and that could be lensed. Chanamé et al. (2001) predicted microlensing events by the SMBH of several stars down to the magnitude of 21–23 mag (see also Alexander & Sternberg 1999 for microlensing rates at lower sensitivities without separating the images).[3] However, they only considered bulge stars, and their adopted limits are much shallower than what will soon be available. Consequently, the lensing of stars behind the SMBH in the Galactic center has not been investigated so far in the context of future telescopes. Hence, the objective of this Letter is to predict whether they will have sufficient sensitivity to detect strongly lensed stars in the background of the SMBH in the Galactic center, and what limiting magnitudes are necessary for this.

We adopt the observing wavelength of 2.2 μm (K-band) and the Vega magnitude system, so we convert AB magnitudes by subtracting 1.85 (Blanton & Roweis 2007).

2. Methods

A star lensed by the SMBH can be identified if the secondary image on the other side of the SMBH is bright enough. The detectability of the secondary image depends on the intrinsic (non-lensed) brightness of the star, the distance of the star behind the SMBH, and the angular separation of the true image (β). Hence, we calculated the total number of detectable lensed stars by integrating along the distance from the SMBH and along the angular separation in the following steps.

1. For each distance we calculated the angular size of the Einstein radius ($\theta_{\rm E}$) assuming the mass of the SMBH of $4.261 \times 10^6\,M_{\odot}$ and the observer-lens distance of $D_{\rm L} = 8.247$ kpc (Gravity Collaboration et al. 2020).
2. We considered only the distances from the SMBH for which the Einstein ring is larger by a factor of 5 than the resolution of a given telescope, so that the separation of the lensed images can be measured. This assumption has little impact on the calculations, because it excludes only very small distances and hence a very small volume. We integrated up to the lens-source distance $D_{\rm LS} = 16$ kpc from the SMBH, which we assume to be the radius of the Milky Way disk.
3. For a given distance from the observer to the star $D_{\rm S} = D_{\rm L} + D_{\rm LS}$ and for a given limiting magnitude of the telescope, we calculated the absolute magnitude above which a secondary image can be detected.
4. We corrected this absolute magnitude for dust extinction in three ways. First, for each star we applied the same correction as for stars orbiting the SMBH of $A_{K,\rm SMBH} = 2.42$ mag (Fritz et al. 2011). This effectively assumes that there is no dust behind the SMBH, so is a lower limit on dust extinction. Second, we assumed that extinction is linear with distance, so for a star 8.247 kpc behind the SMBH the extinction is twice the value measured for the SMBH surroundings. Given that most of the dust along this line of sight is located close to the Galactic center, this likely overestimates the extinction for large distances. Finally, we assumed a more realistic model with dust density decreasing exponentially with the distance from the Galactic center, and the extinction proportional to the integral of this density (Equation (A3) in Appendix A).
5. For each angular separation of the true position of the star and SMBH β, we calculated the amplification factor of the secondary image $\mu_{-} = (u^2 + 2)/(2u\sqrt{u^2 + 4}) - 0.5$, where $u = \beta/\theta_{\rm E}$ (Schneider et al. 1992). The absolute magnitude limit from the previous point was corrected for this amplification. We considered angular separations up to $5\theta_{\rm E}$ at which the secondary image has the flux of only 0.14% of the unlensed star. Most of the detectable lensed stars are located within $2\theta_{\rm E}$, but such wider angles resulted in a non-negligible increase for deep limits.
6. For each angular separation β and for a given distance $D_{\rm S}$ between the observer and the star, we calculated the volume between β and $\beta + d\beta$ and between $D_{\rm S}$ and $D_{\rm S} + dD_{\rm S}$ as $2\pi D_{\rm S}^2\,\beta\,d\beta\,dD_{\rm S}$.
7. In order to estimate the volume number density of stars we used the star luminosity function as measured within 100 pc in the Gaia G filter (Gaia Collaboration et al. 2021). Each G-band absolute magnitude was converted to K-band using main-sequence colors (Pecaut et al. 2012; Pecaut & Mamajek 2013).[4] The result does not change significantly if we use a luminosity function measured directly in the K-band (Equation (3) and table 2 in Mamon & Soneira 1982). Then we assumed that for stars in the disk this luminosity function only applies close to the Solar neighborhood and on the other side of the SMBH with $D_{\rm LS} = D_{\rm L} = 8.247$ kpc and scaled the number density at other distances to reflect an exponential disk, i.e., by a factor $\exp[-(D_{\rm LS} - D_{\rm L})/h_{\rm disk}]$ with a scale length of $h_{\rm disk} = 2.75$ kpc (Zheng et al. 2001). We then considered the bulge applying the model of Dwek et al. (1995), in which the star number density is proportional to $\exp[-0.5(D_{\rm LS}/{\rm kpc})^2]$. The normalization was set so that at the Galaxy center the bulge has the number density a factor of $1.23/1.07 = 1.15$ higher than the disk (table 2 of Batista et al. 2011).
8. To obtain a local number density of detectable stars at a given distance from the SMBH and at a given angular separation, we integrated this (scaled) star luminosity function above the limiting absolute magnitude derived in 5.
9. We multiplied this number density by the volume element derived in 6 and obtained the number of detectable secondary images in this element.
10. We added the contributions of each angular separation and each distance to derive the cumulative number of detectable lensed stars as a function of distance from the SMBH.

We made these calculations for the Extremely Large Telescope (ELT) with the Multi-Adaptive Optics Imaging Camera for Deep Observations (MICADO), Thirty Meter Telescope (TMT) with the Infrared Imaging Spectrograph (IRIS), Giant Magellan Telescope (GMT) with GMT Integral-Field Spectrograph (GMTIFS), James Webb Space Telescope (JWST) with Near Infrared Camera (NIRCam), and Very Large Telescope Interferometer (VLTI) with GRAVITY. We also made the calculations for the parameters

[3] Lensing of stars by the SMBH in the center of M31 was also considered by Bozza et al. (2008).

[4] http://www.pas.rochester.edu/~emamajek/EEM_dwarf_UBVIJHK_colors_Teff.txt

Table 1
Assumed Spatial Resolutions and Limiting Magnitudes (Vega, 5σ) in 1 hr and 5 hr at 2.2 μm

Telescope/Instrument	Resolution (mas)	Sensitivity (mag)	References
ELT/MICADO	11	27.2/28.0	Davies et al. (2010, 2018)[i]
TMT/IRIS	15	27.3/28.2	Larkin et al. (2020); Wright et al. (2010)[ii]
GMT/GMTIFS	22	26.2/27.1	Johns et al. (2012); McGregor et al. (2012)[iii]
JWST/NIRCam	71	27.3/28.2	Perrin et al. (2014)[iv] Pontoppidan et al. (2016)[v]
VLTI/GRAVITY	3	19.0[vi]	Gravity Collaboration et al. (2017) Bozza & Mancini (2012)
Keck or VLT or NTT	50	19.0[vi]	Ghez et al. (2008)

Notes.
[i] https://simcado.readthedocs.io/en/latest/index.html.
[ii] https://www.tmt.org/etc/iris.
[iii] http://www.mso.anu.edu.au/gmtifs/Performance/GMTIFS-Imager-ETC.html.
[iv] https://jwst-docs.stsci.edu/near-infrared-camera/nircam-predicted-performance/nircam-point-spread-functions.
[v] https://jwst-docs.stsci.edu/near-infrared-camera/nircam-predicted-performance/nircam-imaging-sensitivity.
[vi] The most optimistic limit for this instrument.

corresponding to the best existing images taken with the Keck Telescope, Very Large Telescope (VLT), or New Technology Telescope (NTT). The angular resolutions and 5σ limiting magnitudes in 1 and 5 hr hours of integration used in the calculations are shown in Table 1. For ELT, TMT, and GMT the resolution reflects the diffraction limit at 2.2 μm. For 4–8 m class telescopes and for VLTI/GRAVITY, instead of 1 and 5 hr limits we used the most optimistic limit in order to show the maximum number of detectable lensed stars.

3. Results

For each telescope listed in Table 1, Figure 1 presents six cumulative numbers of lensed stars with detectable secondary images, corresponding to three choices of the extinction model (point 4 above), and two choices of the number density model, the disk and bulge (point 7 above). We assumed 5σ limits in 5 hr of integration for this figure, and in 1 hr of integration for Figure B1 in Appendix B. For 4–8 m class telescopes and for VLTI/GRAVITY we show a single panel, because we adopt the same (most optimistic) limiting magnitude. ELT, TMT, GMT, and JWST should detect lensed secondary images of around 100 (60) stars in the disk and 30 (20) stars in the bulge, down to 28 (27) mag (Vega) 5σ limits requiring 5 (1) hr of integration. The number depends mostly on adopted extinction, because it affects mostly larger distances at which the probed volume is larger. Most of the detected stars will be located within 5 kpc behind the SMBH, because of the decreasing number density of stars in the disk.

VLTI/GRAVITY will not be able to see any secondary images of lensed stars, as their expected number is less than 0.1. Similarly, we predict that existing 4–10 m telescopes should not have detected any of such images, consistently with the lack of such discovery using existing images.

Figure 2 shows the number of detectable secondary images of lensed stars as a function of the limiting magnitude. In order to detect several such stars one needs the limit of at least 24 mag.

4. Discussion

We show that with future telescopes it will be possible to look for lensed images of background stars. One would need to identify two sources exactly on the other side of the position of the SMBH, whose spectra and/or colors are identical and whose positions and fluxes satisfy the lensing equation.

The calculations show that sensitivity is a much more important factor to resolve lensed images of background stars than resolution (though sensitivity depends on resolution indirectly due to confusion, see below). Indeed, VLTI/GRAVITY has better resolution than 20–40 m class telescopes, but only the latter will be able to detect secondary images of lensed stars, because they will be 8–9 magnitudes more sensitive. Similarly, JWST/NIRCam has a resolution comparable to the existing images with the Keck telescope, but we predict it to be able to detect secondary images of lensed background stars, due to its improved sensitivity (but see the confusion limitations below).

This is because all considered telescopes do have sufficient resolution to resolve lensed image separation, which is of the order of the Einstein radius. For a background star 1–16 kpc behind the SMBH it is $0\farcs7$–$1\farcs6$. Therefore, limitation is the number of stars that are within such a small angular distance from the SMBH. In the vicinity of the SMBH the number density of stars is so high that several tens of such stars have been detected in the central arcsec; though the lensing signature for them is extremely small. For distances far enough so that the Einstein radius is larger, the number density of stars in the disk is very low. Hence, in order to detect any of them, a very deep image is required in order to probe intrinsically fainter, and hence more numerous, stars.

In these calculations we do not take into account confusion, which in principle is a limiting factor of this analysis. Most of the contribution to confusion will come from stars around the SMBH, because they are more numerous than those in the background or foreground. There are 57 stars within the central arcsec from the SMBH detected down to 19 mag (Figure 1 of Gillessen et al. 2017). In order to estimate the number of fainter stars in this population, first we calculated the absolute magnitudes at the distance of 8.247 kpc (around the SMBH) for 19 mag and the limiting magnitude listed in Table 1 and corrected them for dust extinction of $A_{K,\mathrm{SMBH}} = 2.42$ mag, as above. Then we integrated the luminosity function, obtaining 70 times more stars down to the apparent magnitude of 27–28 mag than to 19 mag, i.e., around 4000 stars brighter than 27–28 mag within the central arcsec. This corresponds to 0.6 stars per ELT beam, 1.0 stars per TMT beam, 2.2 stars per GMT beam, and 23 stars per JWST beam (see Table 1). This means that due to their unprecedented resolution, ELT, TMT, and GMT will only start to be confused at the listed limiting magnitudes toward the Galactic center. JWST will be heavily confused toward the Galactic center, so the possibility to

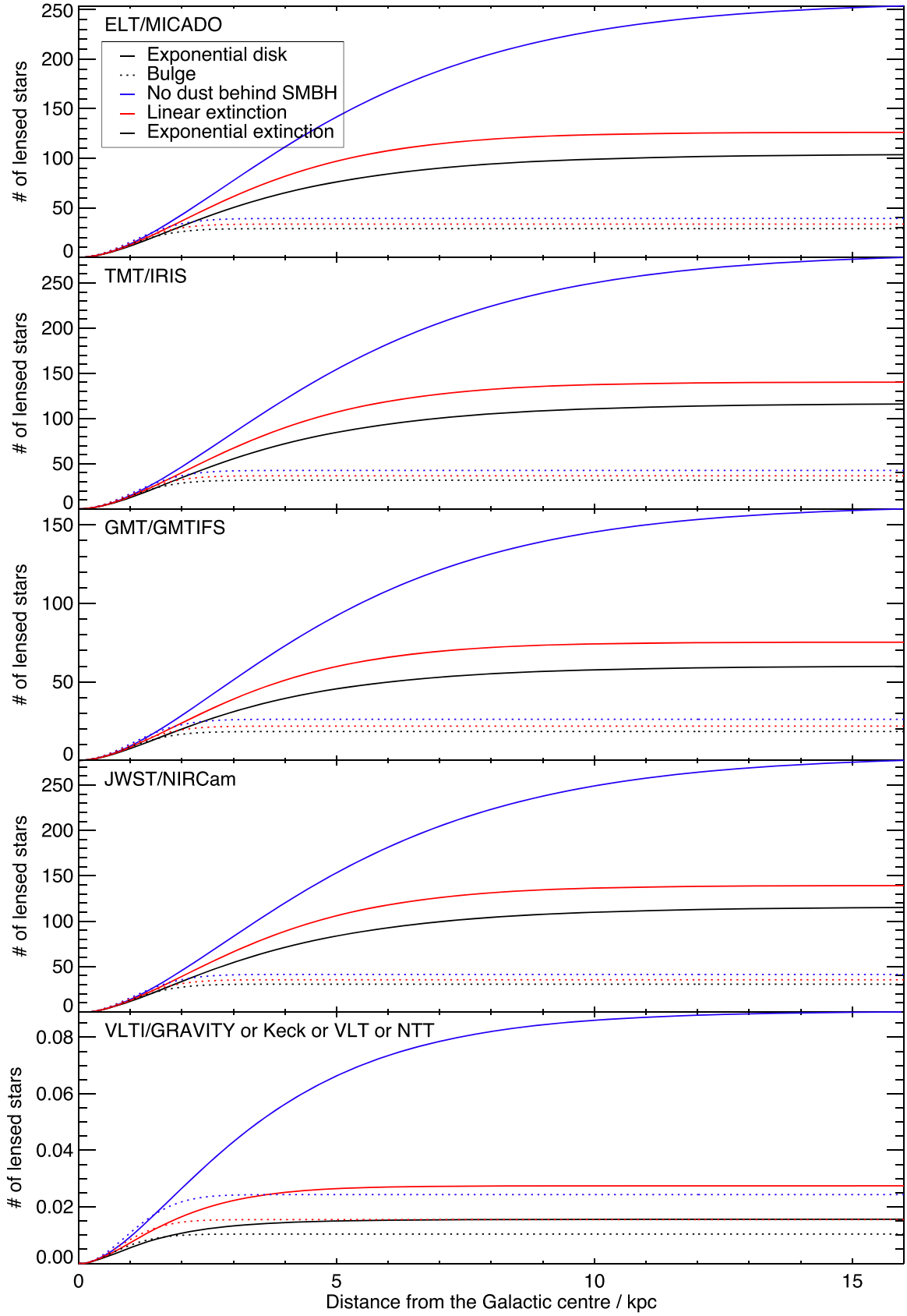

Figure 1. Cumulative number of resolved lensed images of background stars expected to be seen by high-resolution telescopes assuming 5σ limits in 5 hr of integration (Table 1). Solid lines correspond to an exponential disk, whereas dotted lines correspond to the bulge. Blue curves correspond to an optimistic case that the stars will be attenuated in the same way as stars orbiting the SMBH, red curves correspond to dust extinction rising linearly with distance, and black curves correspond to the extinction model in which the dust density decreases exponentially with the distance from the Galactic center (Equation (A3) in Appendix A).

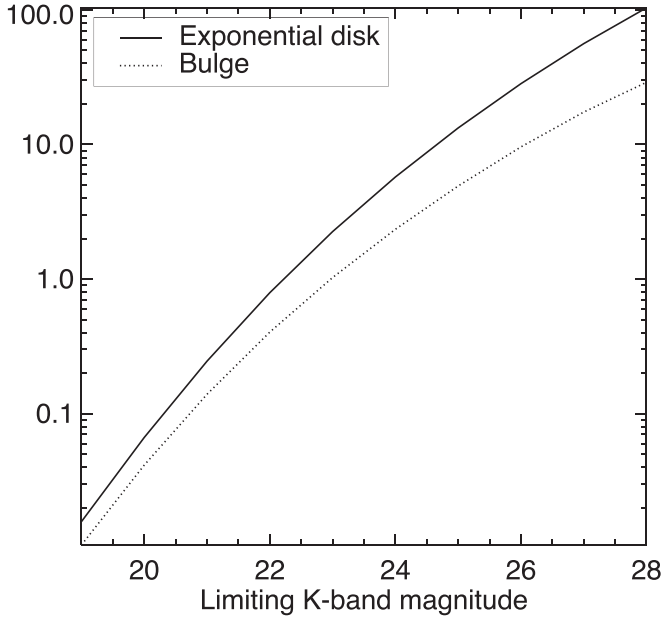

Figure 2. Number of resolved lensed images of background stars expected to be seen by high-resolution telescopes as a function of *K*-band limiting magnitude. The solid line corresponds to an exponential disk, whereas the dotted line corresponds to the bulge. The extinction model in which the dust density decreases exponentially with the distance from the Galactic center was assumed (Equation (A3) in Appendix A).

detect lensed stars in the background will rely on the luck of the existence of a bright star in the background and accurate subtraction of stars around the SMBH. This may also turn out to be possible if the initial mass function in the Galactic center is much more top-heavy, with much fewer faint stars than we calculated above. Otherwise, only the limit of 20 mag will result in one source near the Galactic center per JWST beam. However, at this shallower limit only up to 0.6 lensed background star is expected.

The detection of elongated arcs of lensed background stars will not be possible with any telescope. Taking an optimistic case of a giant with a radius that is 10 times larger than that of the Sun only 0.5 kpc behind the SMBH results in an angular size of 10 μas. Hence, in order to detect the elongation of the image with the best future resolution, the star would need to be stretched by a factor of at least 1000. This requires an extremely accurate alignment of the star with the line toward the SMBH. The tangential magnification for a case of a point lens can be expressed as $\mu_t = x^2/(x^2-1)$, where $x = \theta/\theta_{\rm E}$ and θ is the angular separation of the image and the lens (Schneider et al. 1992). Hence, $\mu_t = 1000$ corresponds to $\theta = 1.001\theta_{\rm E}$, so the image forms almost at the Einstein radius. Using the lens equation for a point lens $\beta = \theta - \theta_{\rm E}^2/\theta$, one obtains the true source separation from the lens of only $\beta = 0.002\theta_{\rm E}$. Considering only the number of stars in such a narrow cone, one gets their total number a factor of 1000^2 lower than for stars within $2\theta_{\rm E}$, calculated above, and hence there will be no stars that close to the SMBH. The increased lensing amplification of the primary image will not help here, because at such small separations from the lens it is almost equal to the amplification of the secondary image, already considered in these calculations.

In order to look for or to confirm a pair of objects as lensed images, one can try to detect their rotation around the SMBH due to relative motion of the source and lens. Proper motion in units of mas per year can be calculated from the linear velocity v in km s^{-1} and distance D in kpc as $v/(4.74D)$. Due to the orbital motion of the Sun around the Galactic center, the SMBH moves with respect to the Sun with a linear velocity of 200 km s^{-1}, whereas a background stars moves with a linear velocity of 400 km s^{-1}, assuming a flat rotation curve. Therefore, for a star $D_{\rm LS} = 1$, 3, 10, 16 kpc behind the SMBH, its relative proper motion with the SMBH is $\mu = 400/(4.74D_{\rm S}) - 200/(4.74 \times D_{\rm L}) = 4$, 2.4, 0.5, and 1.6 mas per year, respectively. The Einstein radius crossing time (Einstein timescale) is $t_E \equiv \theta_{\rm E}/\mu = 170$, 440, 3100, and 1000 yr. Hence, especially for lensed stars not too far behind the SMBH, the comparison of images taken around a decade apart should reveal the rotation of the lensed images.

5. Conclusions

We show that ELT, TMT, and GMT will resolve lensed images of around 100 (60) stars in the disk and 30 (20) stars in the bulge in the background of the SMBH down to 28 (27) mag (Vega) limits at *K*-band, requiring 5 (1) hr of integration. In order to detect several such stars one needs the limit of at least 24 mag. With decade-long monitoring, one can also detect the rotation of the lensed images. JWST will likely be limited by the confusion caused by stars near the Galactic center. If these observations are successful, then, together with the SMBH mass measurement from orbital motions of stars, this will provide a very clean test of general relativity, because both the source and the lens can be considered point-like. For such a test the contribution of stars to the lensing signal will need to be taken into account. Within the central arcsec (0.2 pc) the mass contribution of the SMBH is around 35 times higher than that of stars (Genzel et al. 1997), so this is not problematic, but may hide subtle deviations from general relativity. Moreover, the exact position and mass of the SMBH will be measured in an independent way. This will provide a cross-validation of measurements using orbital motions of stars. The effect of the SMBH spin will be of the order of 4 μas for the first order (Sereno & de Luca 2006), so this will not be constrained by the telescopes considered here. The detection of stretched images of the lensed stars will not be possible because, given extremely small angular sizes of stars, the alignment with the SMBH would need to be better than $0.002\theta_{\rm E}$. The probability that a star happens to be in such a small volume is almost zero.

We wish to thank the referee for useful suggestions, and Joanna Baradziej, Mattia Negrello, Jean Surdej, and Łukasz Wyrzykowski for discussions and comments. M.J.M. acknowledges the discussion with Hong Du on gravitational lensing, which was a prompt to make calculations presented in the Letter. M.J.M. acknowledges the support of the National Science Centre, Poland, through the SONATA BIS grant 2018/30/E/ST9/00208. This research has made use of the NASA/IPAC Extragalactic Database (NED), which is operated by the Jet Propulsion Laboratory, California Institute of Technology, under contract with the National Aeronautics and Space Administration; the WebPlotDigitizer of Ankit Rohatgi (`arohatgi.info/WebPlotDigitizer`) and NASA's Astrophysics Data System Bibliographic Services.

Appendix A
Derivation of the Extinction Profile from Exponential Distribution of Dust

We assumed the exponential Galactic dust density (ρ) model from Sharma et al. (2011, Equation (16)), which in the plane of the disk can be expressed as $\rho = C\exp(-D_{\rm LS}/h)$, where C is

a normalization constant, $D_{\rm LS}$ is the distance from the Galactic center (consistent with the notation above), and $h = 4.2$ kpc is the dust distribution scale length. The extinction for a star at a distance $D_{\rm LS}$ behind the SMBH, therefore, is the extinction measured for stars close to the Galactic center plus the integral of this dust density:

$$A_K = A_{K,\rm SMBH} + \int_0^{D_{\rm LS}} \rho \, dD_{\rm LS} = A_{K,\rm SMBH} + C\left[-h\exp\left(-\frac{D_{\rm LS}}{h}\right)\right]_0^{D_{\rm LS}} = A_{K,\rm SMBH} + Ch\left[1 - \exp\left(-\frac{D_{\rm LS}}{h}\right)\right] \quad \text{(A1)}$$

The value of the constant C can be obtained from the requirement of symmetry that 8.247 kpc behind the SMBH the extinction should be twice as that measured for the Galactic center, i.e. setting $D_{\rm LS} = D_{\rm L}$ and $A_K = 2A_{K,\rm SMBH}$ one obtains

$$C = \frac{A_{K,\rm SMBH}}{h\left[1 - \exp\left(-\frac{D_{\rm L}}{h}\right)\right]} \quad \text{(A2)}$$

and substituting this in Equation (A1), one obtains

$$A_K = A_{K,\rm SMBH}\left[1 + \frac{1 - \exp\left(-\frac{D_{\rm LS}}{h}\right)}{1 - \exp\left(-\frac{D_{\rm L}}{h}\right)}\right] \quad \text{(A3)}$$

This is used for the extinction model in Section 2, point 4 and is compared with the linear and constant models in Figure A1.

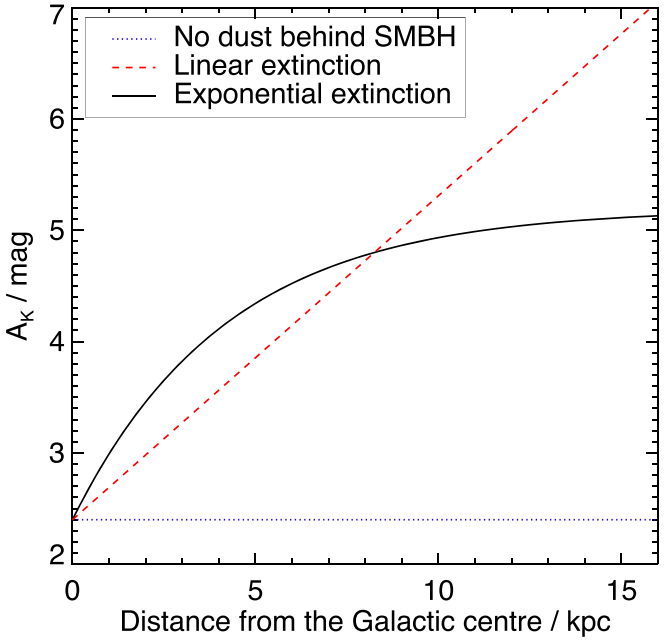

Figure A1. Extinction as a function of distance from the SMBH using the exponential model (black solid line; Equation (A3)), the linear model (red dashed line), and the constant model in which extinction for all stars behind the SMBH is assumed to be the same as that measured for stars orbiting the SMBH (blue dotted line). By the symmetry requirement, 8.247 kpc behind the SMBH the exponential and linear models result in the extinction twice that around the SMBH.

Appendix B
Number of Lensed Stars with 1 hr Limiting Magnitudes

Figure B1 shows the cumulative number of resolved lensed images of background stars expected to be seen by high-resolution telescopes assuming 5σ limits in 1 hr of integration, instead of 5 hr, as shown in Figure 1.

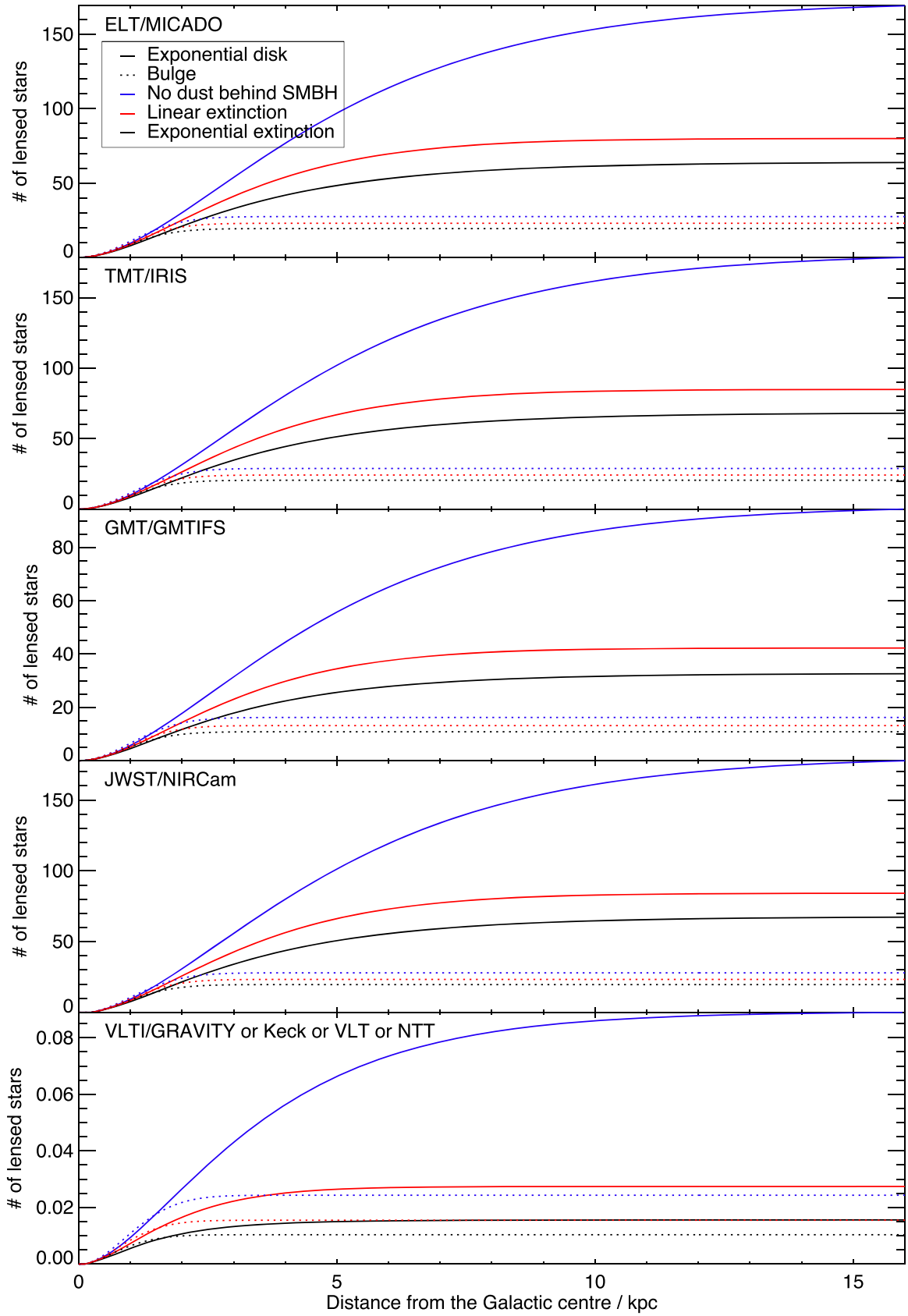

Figure B1. The same as for Figure 1, but for assuming 5σ limits in 1 hr of integration (Table 1).

ORCID iDs

Michał J. Michałowski https://orcid.org/0000-0001-9033-4140
Przemek Mróz https://orcid.org/0000-0001-7016-1692

References

Alexander, T., & Sternberg, A. 1999, ApJ, 520, 137
Batista, V., Gould, A., Dieters, S., et al. 2011, A&A, 529, A102
Bin-Nun, A. Y. 2010, PhRvD, 82, 064009
Blanton, M. R., & Roweis, S. 2007, AJ, 133, 734
Bozza, V., Calchi Novati, S., & Mancini, L. 2008, ApJ, 675, 340
Bozza, V., & Mancini, L. 2004, ApJ, 611, 1045
Bozza, V., & Mancini, L. 2005, ApJ, 627, 790
Bozza, V., & Mancini, L. 2009, ApJ, 696, 701
Bozza, V., & Mancini, L. 2012, ApJ, 753, 56
Chanamé, J., Gould, A., & Miralda-Escudé, J. 2001, ApJ, 563, 793
Chwolson, O. 1924, AN, 221, 329
Davies, R., Ageorges, N., Barl, L., et al. 2010, Proc. SPIE, 7735, 77352A
Davies, R., Alves, J., Clénet, Y., et al. 2018, Proc. SPIE, 10702, 107021S
De Paolis, F., Geralico, A., Ingrosso, G., & Nucita, A. A. 2003, A&A, 409, 809
Diego, J. M., Broadhurst, T., Chen, C., et al. 2016, MNRAS, 456, 356
Dong, S., Mérand, A., Delplancke-Ströbele, F., et al. 2019, ApJ, 871, 70
Dwek, E., Arendt, R. G., Hauser, M. G., et al. 1995, ApJ, 445, 716
Dyson, F. W., Eddington, A. S., & Davidson, C. 1920, RSPTA, 220, 291
Eckart, A., & Genzel, R. 1996, Natur, 383, 415
Eckart, A., & Genzel, R. 1997, MNRAS, 284, 576
Eckart, A., Genzel, R., Ott, T., & Schödel, R. 2002, MNRAS, 331, 917
Einstein, A. 1936, Sci, 84, 506
Fritz, T. K., Gillessen, S., Dodds-Eden, K., et al. 2011, ApJ, 737, 73
Gaia Collaboration, Smart, R. L., Sarro, L. M., et al. 2021, A&A, 649, A6
Genzel, R., Eckart, A., Ott, T., & Eisenhauer, F. 1997, MNRAS, 291, 219
Genzel, R., Pichon, C., Eckart, A., Gerhard, O. E., & Ott, T. 2000, MNRAS, 317, 348
Genzel, R., Thatte, N., Krabbe, A., Kroker, H., & Tacconi-Garman, L. E. 1996, ApJ, 472, 153
Ghez, A. M., Klein, B. L., Morris, M., & Becklin, E. E. 1998, ApJ, 509, 678
Ghez, A. M., Morris, M., Becklin, E. E., Tanner, A., & Kremenek, T. 2000, Natur, 407, 349
Ghez, A. M., Salim, S., Hornstein, S. D., et al. 2005, ApJ, 620, 744
Ghez, A. M., et al. 2008, ApJ, 689, 1044
Gillessen, S., Plewa, P. M., Eisenhauer, F., et al. 2017, ApJ, 837, 30
Goobar, A., Amanullah, R., Kulkarni, S. R., et al. 2017, Sci, 356, 291
Gravity Collaboration, Abuter, R., Accardo, M., et al. 2017, A&A, 602, A94
Gravity Collaboration, Abuter, R., Amorim, A., et al. 2020, A&A, 636, L5
Grillo, C., Karman, W., Suyu, S. H., et al. 2016, ApJ, 822, 78
Jaroszynski, M. 1998, AcA, 48, 413
Jauzac, M., Richard, J., Limousin, M., et al. 2016, MNRAS, 457, 2029
Johns, M., McCarthy, P., Raybould, K., et al. 2012, Proc. SPIE, 8444, 84441H
Kelly, P. L., Rodney, S. A., Treu, T., et al. 2015, Sci, 347, 1123
Kelly, P. L., Rodney, S. A., Treu, T., et al. 2016, ApJL, 819, L8
Kelly, P. L., Diego, J. M., Rodney, S., et al. 2018, NatAs, 2, 334
Larkin, J. E., Wright, S. A., Chisholm, E. M., et al. 2020, Proc. SPIE, 11447, 114471Y
Mamon, G. A., & Soneira, R. M. 1982, ApJ, 255, 181
McGregor, P. J., Bloxham, G. J., Boz, R., et al. 2012, Proc. SPIE, 8446, 84461I
Mróz, P., Udalski, A., Skowron, J., et al. 2017, Natur, 548, 183
Mróz, P., Ryu, Y.-H., Skowron, J., et al. 2018, AJ, 155, 121
Paczynski, B. 1986, ApJ, 304, 1
Paczynski, B. 1996, ARA&A, 34, 419
Pecaut, M. J., & Mamajek, E. E. 2013, ApJS, 208, 9
Pecaut, M. J., Mamajek, E. E., & Bubar, E. J. 2012, ApJ, 746, 154
Perrin, M. D., Sivaramakrishnan, A., Lajoie, C. P., et al. 2014, Proc. SPIE, 9143, 91433X
Pontoppidan, K. M., Pickering, T. E., Laidler, V. G., et al. 2016, Proc. SPIE, 9910, 991016
Rodney, S. A., Brammer, G. B., Pierel, J. D. R., et al. 2021, arXiv:2106.08935
Schneider, P., Ehlers, J., & Falco, E. E. 1992, Gravitational Lenses (Berlin: Springer-Verlag)
Sereno, M., & de Luca, F. 2006, PhRvD, 74, 123009
Sharma, S., Bland-Hawthorn, J., Johnston, K. V., & Binney, J. 2011, ApJ, 730, 3
Udalski, A., Szymanski, M., Kaluzny, J., et al. 1993, AcA, 43, 289
Udalski, A., Jaroszyński, M., Paczyński, B., et al. 2005, ApJL, 628, L109
Wardle, M., & Yusef-Zadeh, F. 1992, ApJL, 387, L65
Wright, S. A., Barton, E. J., Larkin, J. E., et al. 2010, Proc. SPIE, 7735, 77357P
Wyrzykowski, Ł., & Mandel, I. 2020, A&A, 636, A20
Wyrzykowski, Ł., Rynkiewicz, A. E., Skowron, J., et al. 2015, ApJS, 216, 12
Zheng, Z., Flynn, C., Gould, A., Bahcall, J. N., & Salim, S. 2001, ApJ, 555, 393